

Intermolecular interactions of open-shell complexes

Department of Basic Science, The University of Tokyo
Yasuki Endo

By using the supersonic expansion technique, isolated molecules with temperatures from 1 K to 10 K are easily produced. Furthermore, various weakly bound molecular complexes are also produced in the same system. If an appropriate production system is combined with the supersonic technique, it is also possible to produce unstable species and complexes containing unstable species. In our laboratory, we have combined the supersonic jet technique with a pulsed discharge nozzle system to produce unstable species and their complexes. So far, we have studied a number of complexes containing open-shell radicals or molecular ions by Fourier-Transform microwave spectroscopy. Among the species studied, rare-gas–OH and –SH systems are considered to be prototypical systems, since they are simple atom–diatom systems and OH and SH have $^2\Pi$ ground electronic state. It is of interest to understand the behavior of the unquenched spin and orbital angular momenta when these species constitute a complex.

Pure rotational transitions in the cm-wave region are observed for Ne, Ar, and Kr–OH, SH. The spectral patterns observed for these species are those of $^2\Pi$ free radicals, where pure rotational transitions are observed at $5B$, $7B$, ... with parity doublings very much like the Λ -doublings for $^2\Pi$ molecules and the proton hyperfine splittings. However, when they are fitted to a simple Hamiltonian for $^2\Pi$ molecules, a number of higher order terms are required, presumably due to their floppy nature. In order to elucidate the floppy nature of these complexes, analyses using a free-rotor basis have been performed, in which couplings due to the unquenched spin and orbital angular momenta are considered explicitly, and the observed transitions are directly fitted to intermolecular potential surfaces. Initial potential surfaces used for the analyses are obtained by *ab initio* calculations at a level, CCSD(T)/avtz with additional bond functions. Observed transitions

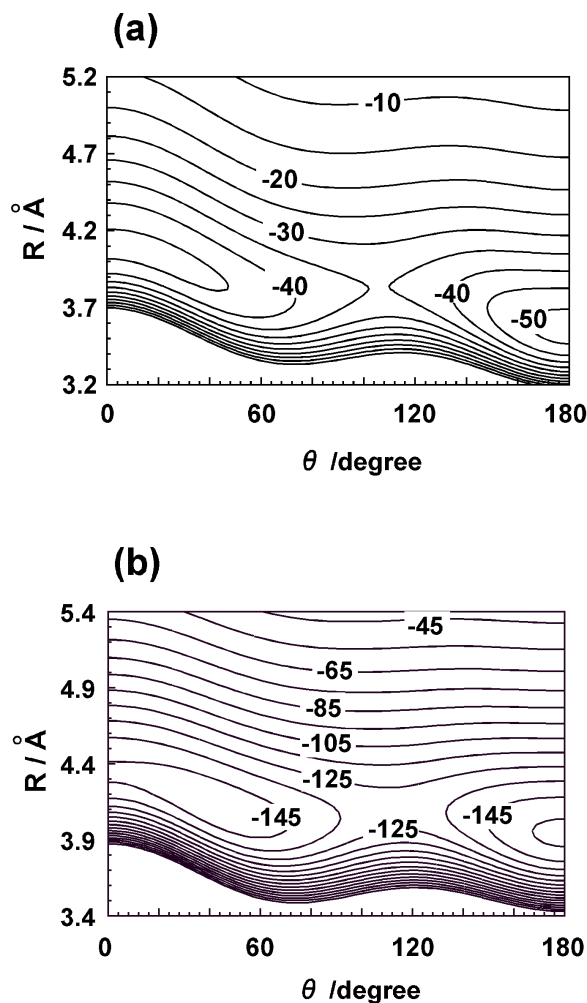


Fig. 1. Potential energy surfaces of Ne-SH and Kr-SH

for all the observed species are fitted within the experimental errors, less than 10 KHz. The determined potential energy surfaces for Ne-SH and Kr-SH are shown in Fig. 1.

Ground electronic state of rare-gas-OH and SH systems are characterized by a large spin-splitting due to the spin-orbit interaction as seen in usual $^2\Pi$ molecules. However, each of the spin component is further split into different P -levels, where P is a quantum number denoting the projection of Ω (for atom-diatom

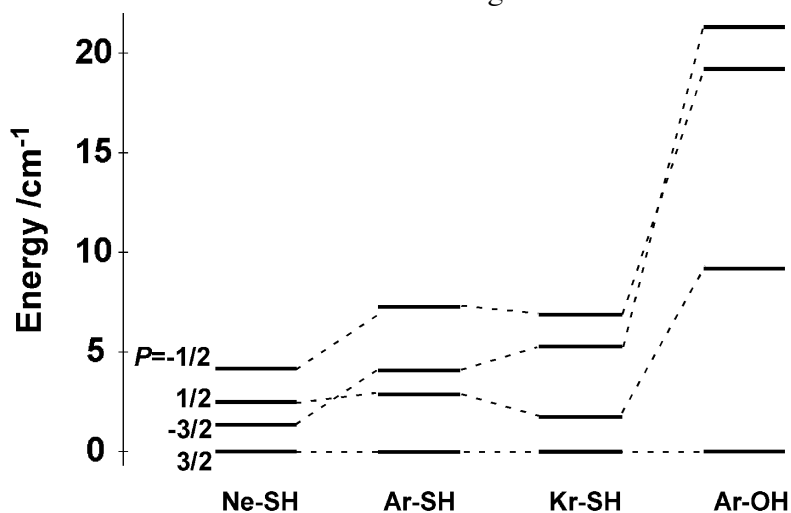


Fig. 2. Energy diagram of P -levels

systems it is usually denoted as ω) onto the intermolecular axis. Thus, the $^2\Pi_{3/2}$ component splits into four components with $P=3/2$, $1/2$, $-1/2$, and $-3/2$ as shown in Fig. 2. It was found that the $P=3/2$ state is the lowest for all the species studied, and pure rotational transitions within the $P=3/2$ state are observed by FTMW spectroscopy. However, relative order and their spacings are quite different among the species observed. For the SH complexes, anisotropies of the potentials are smaller than those of the OH complexes, so that the spacings are much smaller. It is thus possible to observe transitions to different P levels for SH complexes since the spacings are predicted to be only a few cm^{-1} . In order to observe these transitions, we have developed a new double resonance technique, where mm-wave transitions are observed as a change of the free induction decay (FID) signals for the FTMW spectrometer. Observed double resonance transitions are shown in Fig. 3. It was found that the free rotor analyses have predicted the spacings between the $P=3/2$ and $1/2$ states fairly accurately, showing that the potentials determined by the rotational transitions in the $P=3/2$ state are reliable, for Ar-SH and Kr-SH. Analyses including the data obtained by the double resonance technique are now in progress.

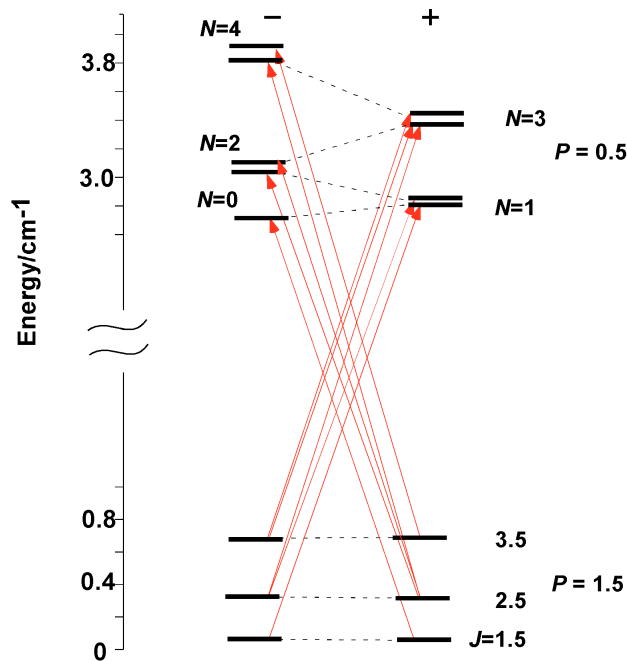


Fig. 3. Observed double resonance transitions